VIP Charge Transport Very Important Paper

International Edition: DOI: 10.1002/anie.201913344
German Edition: DOI: 10.1002/ange.201913344

Structure-Independent Conductance of Thiophene-Based Single-Stacking Junctions

Xiaohui Li[+], Qingqing Wu[+], Jie Bai[+], Songjun Hou, Wenlin Jiang, Chun Tang, Hang Song, Xiaojuan Huang, Jueting Zheng, Yang Yang, Junyang Liu, Yong Hu, Jia Shi, Zitong Liu, Colin J. Lambert,* Deqing Zhang,* and Wenjing Hong**

Abstract: *The experimental investigation of intermolecular charge transport in π-conjugated materials is challenging. Herein, we describe the investigation of charge transport through intermolecular and intramolecular paths in single-molecule and single-stacking thiophene junctions by the mechanically controllable break junction (MCBJ) technique. We found that the ability for intermolecular charge transport through different single-stacking junctions was approximately independent of the molecular structure, which contrasts with the strong length dependence of conductance in single-molecule junctions with the same building blocks, and the dominant charge-transport path of molecules with two anchors transited from an intramolecular to an intermolecular path when the degree of conjugation increased. An increase in conjugation further led to higher binding probability owing to the variation in binding energies, as supported by DFT calculations.*

Introduction

The unique electronic properties of organic π-conjugated materials lead to various applications in flexible and stretchable, light-weight devices for skinlike or wearable electronics, the internet of things, and flexible displays, among others.[1] In macroscopic π-conjugated materials, intermolecular charge transport is widely considered to be the limiting step for electronic processes,[2] owing to their weak dielectric constants and strong electron–phonon interactions, as well as their disordered microscopic structures. Although substantial studies have been carried out to understand the intermolecular charge transport,[2d,3] a quantitative description of charge transport still remains challenging. Until now insight into the charge transport has mostly been gained from theoretical calculations.[2a,c,4] To investigate the role of intermolecular interactions in charge transport, mechanically controllable break junction (MCBJ) studies have demonstrated that charge transport through intermolecular paths provides much lower conductance than that through intramolecular paths in oligophenylene ethynylenes (OPEs),[5] thus suggesting that the single-molecule break junction may offer new insight to overcome long-standing challenges.

Among π-conjugated materials, thiophene derivatives have attracted intense attention for organic electronic devices and molecular electronics owing to their outstanding electronic and optical properties.[6] Understanding the intrinsic charge transport through thiophene derivatives at the molecular level is essential for designing high-performance functional organic materials and devices. Until now, several groups have studied the intramolecular charge transport through thiophene derivatives on the basis of the corresponding single-molecule junctions.[7] However, the intermolecular charge transport through thiophene derivatives, which plays a vital role in the ultimate charge-carrier mobility, has not been studied previously.

In this study, we investigated the intermolecular charge-transport properties of single-molecule and single-stacking thiophene junctions using the MCBJ technique. It was found that thiophene molecules containing only one thiomethyl (−SMe) anchoring group could form single-stacking junctions with measurable conductance. Unexpectedly, the conductance of single-stacking junctions was approximately constant with different conjugation patterns, whereas the probability to form single-stacking junctions improved as the conjugation region was increased, thus indicating that the dynamic formation process provides the driving forces for their charge-transport ability. Moreover, on the basis of the detectable conductance of thiophene-based single-stacking junctions, we explored the intermolecular and intramolecular charge transport through thiophene derivatives at the single-molecule level, demonstrating that intermolecular and intramolecular charge transport can be distinguished and investigated by the MCBJ technique. We found that intermolecular charge transport could be more efficient than intramolecular

[*] X. H. Li,[+] J. Bai,[+] C. Tang, H. Song, X. J. Huang, J. T. Zheng, Y. Yang, J. Y. Liu, Y. Hu, J. Shi, Prof. W. J. Hong
State Key Laboratory of Physical Chemistry of Solid Surfaces, iChEM
College of Chemistry and Chemical Engineering, Xiamen University
Siming South Road, Xiamen (China)
E-mail: whong@xmu.edu.cn

Q. Q. Wu,[+] S. J. Hou, Prof. C. J. Lambert
Department of Physics, Lancaster University
Lancaster LA1 4YB (UK)
E-mail: c.lambert@lancaster.ac.uk

W. L. Jiang, Z. T. Liu, D. Q. Zhang
Beijing National Laboratory for Molecular Sciences
CAS Key Laboratory of Organic Solids, Institute of Chemistry
Chinese Academy of Sciences
Zhongguancun North First Street 2, Beijing (China)
E-mail: zitong_@iccas.ac.cn
dqzhang@iccas.ac.cn

[+] These authors contributed equally to this work.

Supporting information and the ORCID identification number(s) for the author(s) of this article can be found under: https://doi.org/10.1002/anie.201913344.

charge transport in thiophene derivatives and that the dominant charge-transport path transitioned from intramolecular to intermolecular when the conjugation increased. Our findings provide clear evidence that intermolecular, rather than intramolecular, charge transport could be the dominant conductance path for organic materials with a large π-conjugation pattern.

Results and Discussion

The conductance of molecular junctions was characterized using the MCBJ technique in solution (THF/1,3,5-trimethylbenzene 1:4, v/v) with/without target molecules (0.1 mM) at a bias voltage of 0.1 V (Figure 1A). Briefly, the

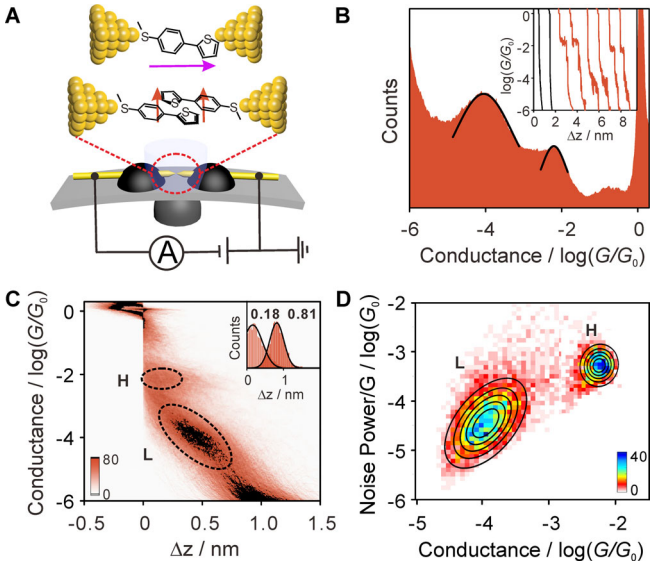

Figure 1. Conductance measurement of molecular junctions. A) Illustration of the MCBJ technique with a single-molecule **S-T1** junction (top) and a single-stacking **S-T1** junction (bottom). B) 1D conductance histograms and typical conductance–displacement traces (inset) of **S-T1** (red) and solvent (black). C) 2D conductance histogram and the relative stretching displacement histograms from $10^{-0.3}$ to $10^{-2.8}$ G_0 of the H state ((0.18 ± 0.03) nm, inset) and $10^{-0.3}$ to $10^{-5.0}$ G_0 of the L state ((0.81 ± 0.02) nm, inset). The error bars were determined from the variation of the relative stretching displacement values in three independent conductance measurements. D) 2D histogram of normalized flicker noise power versus average conductance of **S-T1**.

breaking and closing process between two electrodes was performed by the controllable bending of notched gold-wire chips. In this way, the molecular junctions were created by repeatedly breaking and forming the gold–gold atomic contacts. To investigate the charge transport through a π-stacked thiophene dimer, we used the molecule **S-T1** with only one −SMe terminus to form a single-stacking junction through intermolecular interactions, with each −SMe group of the dimer coupled to a gold electrode (Figure 1A).

Figure 1B shows several typical conductance–displacement traces of **S-T1** (red) and the solvent without molecules (black). Unlike in direct tunneling traces obtained for the solvent, the conductance indicated by the red traces decreases to two well-defined molecular plateaus after the rupture of the last gold–gold atomic contact at 1 G_0 ($G_0 = 2e^2/h$),[8] thus suggesting the formation of two distinct molecular junctions for **S-T1**. The high-conductance (H) and low-conductance (L) plateaus can appear individually or together. We explored the correlation of the H and L states statistically by 2D cross-correlation analysis (see Figure S5A in the Supporting Information).[9] A negatively correlated region centered at [$10^{-2.2}$ G_0, $10^{-4.0}$ G_0] and [$10^{-4.0}$ G_0, $10^{-2.2}$ G_0] was found for **S-T1**, thus indicating that the two conductance states appear competitively in most cases (see the Supporting Information for details). A one-dimensional (1D) conductance histogram was generated to determine the most likely conductance, and two evident conductance peaks were obtained (Figure 1B). The H peak centered at $10^{-2.18\pm0.04}$ G_0 ((517.1 ± 44.0) nS) displays a narrow distribution and is 68 times higher than the L peak ($10^{-4.02\pm0.11}$ G_0, (7.5 ± 2.0) nS) with a broad distribution. We speculated that the H peak corresponds to the single-molecule junctions bridged by −SMe[10] and thienyl[11] groups (Figure 1A, top), and the L peak corresponds to the single-stacking junctions between π-stacked dimers (Figure 1A, bottom). The broader peak width of the L peak is related to more degrees of freedom during the stretching process as introduced by π-stacked dimers.

To reveal more information about the stretching process statistically, we constructed two-dimensional (2D) conductance histograms by collecting thousands of individual traces without data selection (Figure 1C). The H intensity cloud remained almost flat during the stretching process, whereas the slope of the L intensity cloud decreased significantly, thus suggesting that the conductance of single-stacking junctions highly depends on the stacking configuration.[12] Furthermore, the stretching distance of the H state was much shorter than that of the L state (Figure 1C, inset). Considering the snap-back distance of 0.5 nm[12] (see the Supporting Information for details), the stretching distance of the H state was (0.68 ± 0.03) nm, which is comparable with the **S-T1** molecular length calculated from theoretical simulations (see Table S1 in the Supporting Information). In comparison, the stretching distance of the L state was almost twice that of the H state ((1.31 ± 0.02) nm), in accordance with the longer length of the single-stacking junction of the **S-T1** dimer.

To further verify our hypothesis, we confirmed the electronic coupling types of the two conductance states by flicker noise analysis[13] (see Section 2.3 of the Supporting Information for details). As shown in Figure 1D, the noise power scales as $G^{1.1}$ for the H state and as $G^{1.8}$ for the L state, corresponding to through-bond coupling in the H state of single-molecule junctions and through-space coupling in the L state of single-stacking junctions, which agrees well with our hypothesis. The phenomenon is different to that observed for short oligothiophene with iodide anchors at both ends, which tend to lie flat on an Au electrode and form single-molecule junctions through metal–π interactions, as reported by Xiang et al.[7a] A possible reason is that the thiophene molecules with −SMe on only one side tend to stand on the gold electrode rather than lie flat, thus facilitating the formation of a gold–sulfur donor–acceptor bond by the S atom of the thiophene

ring and the gold electrode during the stretching process, which is supported by the stretching distance and flicker noise analysis. These results indicate that the interactions between thiophene rings are strong enough to form the single-stacking junctions, and the intermolecular charge-transport ability of single-stacking junctions based on **S-T1** is much lower than that of the corresponding single-molecule junction, as reported before for an OPE system.[5a]

To address how intermolecular charge transport through thiophene-stacking junctions varies according to the conjugation pattern, we synthesized another three kinds of thiophene-based derivatives: i) molecules with an increased number of thiophene units (**S-T2**, **S-T3**), ii) a fused thiophene with a more rigid structure (**S-TTT**), and iii) molecules with substituent groups on the thiophene ring (**S-T1-Cl**, **S-T1-Br**). Figure 2 shows the 1D conductance histograms of the six thiophene derivatives. As shown in Figure 2A, **S-T2** and **S-T3** with two and three thiophene units each had only one conductance peak, and the conductance varied slightly at $10^{-4.05\pm0.04}\,G_0$ ((7.0 ± 0.6) nS) and $10^{-3.91\pm0.03}\,G_0$ ((9.6 ± 0.7) nS) as compared to **S-T1** ($10^{-4.02\pm0.11}\,G_0$). The stretching distances of these molecular junctions are significantly longer than the calculated molecular lengths (see Figure S3A,B and Table S1). Furthermore, flicker noise analysis showed that the noise power scaled as $G^{2.0}$ for **S-T2** and as $G^{1.6}$ for **S-T3** (see Figure S3C,D), which are indicative of through-space coupling through **S-T2** or **S-T3** dimers. Accordingly, we attribute the conductance peaks around $10^{-4.0}\,G_0$ to single-stacking junctions of **S-T2** and **S-T3**. The absence of single-molecule junctions is possibly caused by the weak competitiveness as compared to single-stacking junctions as the molecular conjugation length increases, since the presence of single-molecule junctions and single-stacking junctions is competitive as discussed above.

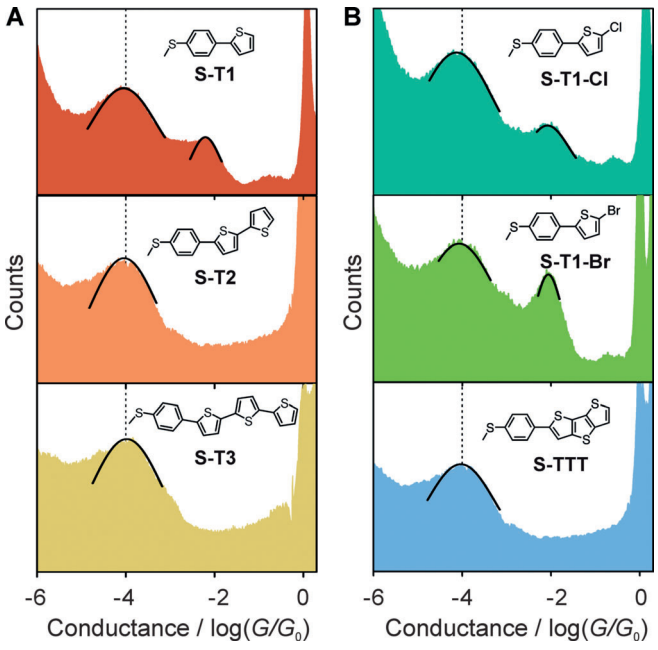

Figure 2. Investigation of intermolecular charge transport of thiophene derivatives. A) Molecular structures and 1D conductance histograms of molecules **S-T1** ($10^{-4.02\pm0.11}\,G_0$), **S-T2** ($10^{-4.05\pm0.04}\,G_0$), and **S-T3** ($10^{-3.91\pm0.03}\,G_0$) at 0.1 mM. B) Molecular structures and corresponding 1D conductance histograms of **S-T1-Cl** ($10^{-4.01\pm0.09}$ and $10^{-2.01\pm0.03}\,G_0$), **S-T1-Br** ($10^{-4.07\pm0.02}$ and $10^{-2.09\pm0.02}\,G_0$), and **S-TTT** ($10^{-3.97\pm0.05}\,G_0$). Details of the analysis can be found in Figure S6.

Next, the effects of substituents and different conjugation patterns on intermolecular charge transport were investigated. Interestingly, single-stacking junctions of **S-T1** derivatives with substituent groups, that is, **S-T1-Cl** with chlorine ($10^{-4.01\pm0.09}\,G_0$, (7.7 ± 1.6) nS) and **S-T1-Br** with bromine ($10^{-4.07\pm0.02}\,G_0$, (6.6 ± 0.4) nS), and the fused-ring thiophene **S-TTT** ($10^{-3.97\pm0.05}\,G_0$, (8.3 ± 0.9) nS) also showed similar conductance values centered at $10^{-4.0}\,G_0$ (Figure 2B), thus suggesting that charge-transport ability through the single-stacking junctions based on thiophene units is nearly independent of the conjugation pattern.

To explore the universality of the above findings, we extended the studies to benzene-based junctions with a fused phenyl (compound **S-P1**), naphthyl (compound **S-P2**), or anthryl ring (compound **S-P3**; see Figure S6). The conductance of **S-P1** ($10^{-4.34\pm0.01}\,G_0$, (3.5 ± 0.05) nS) and **S-P2** ($10^{-4.42\pm0}\times10\,G_0$, (3.0 ± 0.7) nS) were similar, but there was an apparent decrease for **S-P3** ($10^{-4.60\pm0.08}\,G_0$, (1.9 ± 0.3) nS). As compared to the thiophene system, the intermolecular charge-transport ability of single-stacking junctions based on benzene units was generally lower. These results indicate that the thiophene-based single-stacking junctions exhibit excellent intermolecular charge-transport ability, which is also more tolerant to variation of the molecular architecture.

Even though the conductance values of the single-stacking junctions remained nearly structure-independent, the conductance peaks, especially for benzene-based junctions (see Figures S6D–F), became more pronounced as the conjugation region increased. This trend suggests that the structure of the conjugated core plays a role in the dynamic formation of single-stacking junctions. To evaluate the role of conjugation patterns in the intermolecular interactions quantitatively, we constructed displacement distribution histograms for **S-T1**, **S-T2**, and **S-T3** in the conductance range between $10^{-(Gm-1)}$ and $10^{-(Gm+1)}\,G_0$ (see the Supporting Information for details). The displacement distributions centered at 0.36 nm represent the direct tunneling feature without molecular junctions (T), whereas the longer displacement distributions are assigned to single-stacking junctions (J; Figure 3A). The area ratios of the relative stretching distance histograms obtained by Gaussian fitting reveal the formation percentage of single-stacking junctions. It was found that the stacking probability of thiophene-based junctions started at (80 ± 0.9)% for **S-T1** and increased slightly to (83 ± 1.0)% for **S-T2** and (95 ± 1.6)% for **S-T3** (Figure 3B), as attributed to the effective π–π stacking interactions arising from the increasing conjugation. By contrast, the stacking probability of molecule **S-P1** was determined to be only (62 ± 2.7)%. When the π-conjugated core was expanded to yield the anthryl derivative **S-P3**, the stacking probability increased to a value as high as (91 ± 3.9)% (Figure 3B).

The generally higher stacking probabilities of thiophene-based junctions are enhanced by the introduction of sulfur atoms, which introduce additional S–S[14] and S–π interactions[15] and increase the stability of the single-stacking

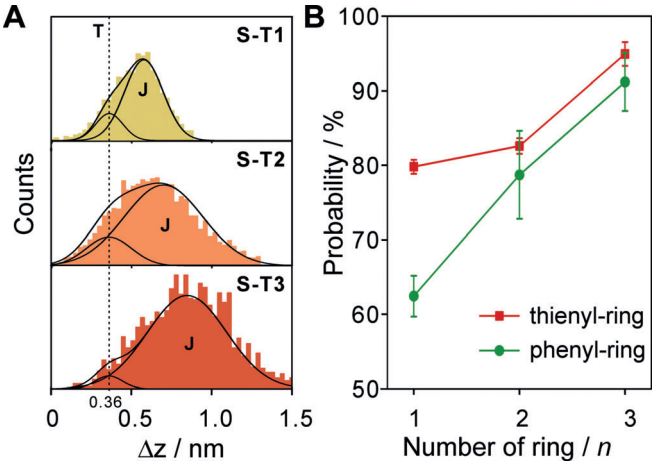

Figure 3. Structure dependence of the stacking probability. A) Displacement distribution histograms of single-stacking junctions with molecules **S-T1**, **S-T2**, and **S-T3** from $10^{-(Gm-1)}$ to $10^{-(Gm+1)}$ G_0. We refer to the direct tunneling feature as "T" (dashed black line) and the molecular junction feature as "J". B) Stacking probability as a function of the number of aromatic rings, *n*, connected to the −SMe anchor group, without regard to *p*-phenylene. The error bars were determined from the variation of the stacking probability in three independent conductance measurements.

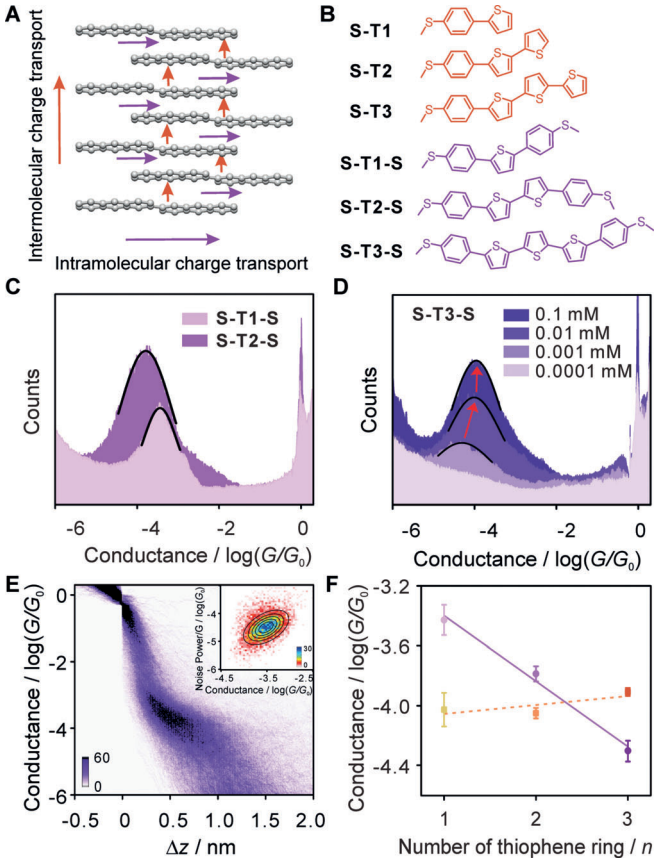

Figure 4. Investigation of intermolecular and intramolecular charge transport. A) Illustration of intramolecular and intermolecular charge transport. B) Molecular structures used for comparison. C) 1D conductance histograms of **S-T1-S** and **S-T2-S**. D) 1D conductance histograms of **S-T3-S** at different concentrations. E) 2D conductance histogram and 2D histogram of normalized flicker noise power versus average conductance of **S-T3-S** at 0.1 mM. F) Conductance as a function of the number of thiophene rings, *n*, in single-molecule (solid line) and single-stacking junctions (dotted line) at 0.1 mM, or for **S-T3-S** at 0.001 mM. The error bars were determined from the variation of the most probable conductance values in three independent conductance measurements.

junctions. Stacking probability analysis, together with the constant conductance of single-stacking junctions, provides essential insight into the charge-transport enhancement induced by aggregation in organic semiconductors.[3b] Such aggregation increases the formation probability of short-range π-stacked units and subsequently leads to the enhanced charge transport through π-conjugated materials.

As discussed above, charge transport through thiophene-based single-stacking junctions can be detected using the MCBJ technique, thus providing the opportunity to explore intermolecular and intramolecular charge transport (as shown in Figure 4A) through thiophene derivatives at the single-molecule level. To distinguish intermolecular and intramolecular charge transport, our approach was to investigate charge transport through single-stacking and single-molecule junctions with the same thiophene backbone. The molecules in orange in Figure 4B with only one −SMe terminus were employed to form a single-stacking junction as we have discussed, and intramolecular charge transport through the thiophene backbones was investigated using the molecules in purple with the two −SMe termini as bridges between two gold electrodes.

Unlike the structure-independent conductance of single-staking junctions, the conductance of single-molecule junctions decreased significantly from $10^{-3.43\pm0}\times10\,G_0$ ((29.5 ± 6.9 nS), **S-T1-S**) to $10^{-3.78\pm0.05}\,G_0$ ((12.8 ± 0.2) nS, **S-T2-S**; Figure 4C). For **S-T3-S**, significant concentration dependence was observed, with the conductance increasing from $10^{-4.31\pm0.07}\,G_0$ ((3.8 ± 0.6) nS, 0.001 mM) to $10^{-3.89\pm0.05}\,G_0$ ((9.9 ± 1.2) nS, 0.1 mM; Figure 4D). Figure 4E shows the 2D conductance–distance histogram and electronic coupling through flicker noise analysis of **S-T3-S** at 0.1 mM. The noise power scales as $G^{1.6}$ for **S-T3-S**, thus indicating that the charge transport through **S-T3-S** occurred predominantly in a through-space manner at higher concentration. Furthermore, concentration-dependent fluorescence emission spectra of **S-T3-S** revealed that the monomer prevailed below 0.01 mM and began to aggregate from 0.01 to 0.1 mM (see Figure S8), thus indicating that the conductance at a low concentration of 0.001 mM and a high concentration of 0.1 mM could be assigned to single-molecule junctions and single-stacking junctions, respectively. Therefore, **S-T3-S** will undergo the transition from single-molecule to single-stacking at higher concentration.

The concentration-dependent behavior of **S-T3-S** found in this study is different from that of oligothiophene reported by Capozzi et al.[7b] The discrepancy can possibly be attributed to the structural differences between oligothiophene and the thiophene/phenylene co-oligomer, which forms intermolecular complexes with increasing concentration.[16] However, no concentration dependence was observed for short molecules, such as **S-T2-S**, and the corresponding noise power scaled as

$G^{1.2}$ for 0.1 mM. These results demonstrate that the charge-transport paths could be controlled to be intermolecular or intramolecular by rational molecular design. Extended conjugation is more favorable for the generation of intermolecular charge transport because of the strong molecular interactions.

Figure 4F summarizes the conductance evolution of single-stacking (dashed line) and single-molecule junctions (solid line) varying with molecular length. The single-molecule conductance of **S-T1-S**, **S-T2-S**, and **S-T3-S** decreases exponentially with an increasing number of thiophene units, which is consistent with the conductance decay of single-molecule oligothiophene junctions[7a,b] and DFT calculations (see Figure S11J). In contrast, the conductance of single-stacking junctions remains almost unchanged. When the molecules are relatively short, the conductance of single-stacking junctions is lower than that of the corresponding single-molecule junctions. However, there is a reversal when the conjugation pattern increases to three thiophene rings, whereby the single-stacking conductance of **S-T3** is approximately 200% higher than the single-molecule conductance of **S-T3-S**, thus suggesting that intermolecular charge transport is even more efficient than intramolecular charge transport with large conjugation patterns. The conductance transition originates from the significant conductance decay with the length of intramolecular charge transport and the near length independence of intermolecular charge transport through single-stacking junctions. Such low length decay of through-space charge transport was also found in single-stacking junctions based on benzene (see Figure S7P) and a previous study on π-folded molecular junctions based on anthracene moieties.[17]

To understand the dominance of intermolecular charge transport, we further calculated the transmission function $T(E)$ describing electrons of energy E passing from one electrode to the other using a combination of the software package SIESTA[18] based on ab initio DFT and the quantum transport code Gollum.[19] To model the evolution of the single-stacking junction, two target molecules were initially attached to two gold pyramidal-shaped electrodes, as shown in Figure 5A (top) for molecule **S-T1**. Then, the electrode spacing d was increased gradually in increments of 0.05 nm, from $d = 1.52$ nm to the break-off distance of the π-stacked dimers (Figure 5A, bottom). Figure 5B shows examples of the transmission functions of a single-stacking **S-T1** junction at various stages of the stretching simulation (see Figure S11A for details). The transmission curves demonstrate that both constructive and destructive quantum interference are observed during the stretching process. However, only the high conductance state was obtained in our experiments owing to the relatively high stretching rate, which is in accordance with the previous report.[20] Figure 5C shows the room-temperature conductance evolutions during stretching as obtained from the transmission coefficients at the Fermi level estimated by DFT. During junction stretching, oscillations in conductance occur, as theoretically predicted[21] and measured[20] in previous studies, and the conductance histograms (Figure 5C, inset) suggest that the calculated conductance of dimers is approximately $10^{-5.0}\,G_0$. The similar

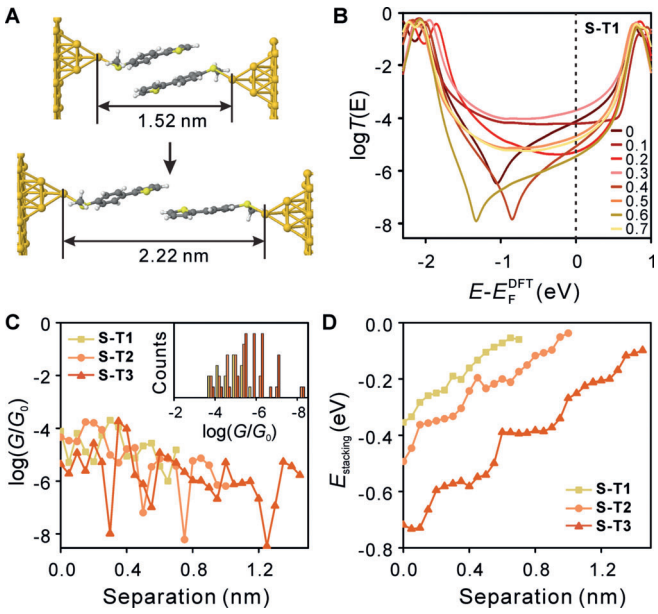

Figure 5. Transmission curves and stacking energies calculated between single-stacking junctions. A) Stretching simulation from full-stacking (1.52 nm) to zero-stacking (2.22 nm) of the **S-T1** junction. B) Representative transmission curves of single-stacking **S-T1** junctions at different separation distances between the two parts of the π-stacked dimer, where "0" corresponds to the initial full-stacking state, and the distance increases in increments of 0.1 nm up to the zero-stacking state ("0.7"). C) Corresponding conductance evolutions obtained from the transmission coefficients at the Fermi level versus the separation distance of **S-T1**, **S-T2**, and **S-T3**, and the conductance histograms (inset) with a bin size of 0.4 $\log(G/G_0)$. D) Stacking energies calculated between dimers of molecules **S-T1**, **S-T2**, and **S-T3** versus the relative separation distance between two gold electrodes.

conductance regions among different derivatives and variation tendency provide qualitative theoretical evidence for the conductance consistency observed experimentally.

To investigate the effect of molecular structure on the stacking probability, we also calculated the stacking energy of the dimers in the junctions at each increment of the stretching process. The binding energies (see the Supporting Information) decrease almost monotonically as the separation distance d increases (Figure 5D). The initial binding energy for thiophene-based **S-T1** is lower than that of **S-T2** and **S-T3**, because the area of the initial π–π overlap area of **S-T1** is smaller than the initial overlap areas of **S-T2** and **S-T3**. This feature supports our experimental results, indicating that the binding probability of **S-T1** is lower than that of **S-T2** and **S-T3**. Since the measured stacking probabilities follow the trends observed for the initial binding energies, it is inferred that the structure dependence of the stacking probability originates from variations in the binding energies of the π–π stacking.

Conclusion

In conclusion, we investigated the intermolecular and intramolecular charge-transport properties of single-molecule

and single-stacking thiophene junctions using the MCBJ technique. We demonstrated that the conductance of thiophene-based single-stacking junctions is nearly independent of the conjugation pattern, and the dominant charge-transport path transits from an intramolecular to an intermolecular path when the conjugated region increased. We also found that the major effect of the increased conjugated region was to improve the dynamic formation of the single-stacking junction rather than its intrinsic conductance at a molecular level. The results were further confirmed by theoretical calculations, which predict similar conductance tendencies and different binding energies of the single-stacking junctions. Our results not only provide a fundamental understanding of the structure–property relationship but also offer fundamental insight into how, from a single-molecule perspective, microscopic charge transport in highly disordered materials enables existing aggregation to increase the formation probability of intermolecular charge-transport channels. We believe our findings will inspire various new design strategies for the fabrication of high-performance organic devices through molecular engineering of intermolecular interactions.

Acknowledgements

This research was supported by the National Natural Science Foundation of China (Nos. 21933012, 21722305, 21673195, 21703188), the National Key R&D Program of China (2017YFA0204902), the FET Open project 767187-QuIET, the EU project BAC-TO-FUEL, UK EPSRC grants EP/N017188/1, EP/P027156/1, and EP/N03337X/1 for funding instrumentation used in Lancaster, and the Youth Innovation Promotion Association CAS (No. 2015024).

Conflict of interest

The authors declare no conflict of interest.

Keywords: conducting materials · conjugation · mechanically controllable break junctions · intermolecular charge transport · thiophene junctions

[1] a) S. Wang, J. Xu, W. Wang, G.-J. N. Wang, R. Rastak, F. Molina-Lopez, J. W. Chung, S. Niu, V. R. Feig, J. Lopez, T. Lei, S.-K. Kwon, Y. Kim, A. M. Foudeh, A. Ehrlich, A. Gasperini, Y. Yun, B. Murmann, J. B. H. Tok, Z. Bao, *Nature* **2018**, *555*, 83 – 88; b) C. Jiang, H. W. Choi, X. Cheng, H. Ma, D. Hasko, A. Nathan, *Science* **2019**, *363*, 719 – 723; c) H. Sirringhaus, *Adv. Mater.* **2014**, *26*, 1319 – 1335.

[2] a) V. Coropceanu, J. Cornil, D. A. da Silva Filho, Y. Olivier, R. Silbey, J.-L. Brédas, *Chem. Rev.* **2007**, *107*, 926 – 952; b) Y. Diao, B. C. K. Tee, G. Giri, J. Xu, D. H. Kim, H. A. Becerril, R. M. Stoltenberg, T. H. Lee, G. Xue, S. C. B. Mannsfeld, Z. Bao, *Nat. Mater.* **2013**, *12*, 665 – 671; c) Z. Shuai, H. Geng, W. Xu, Y. Liao, J.-M. André, *Chem. Soc. Rev.* **2014**, *43*, 2662 – 2679; d) C. Wang, H. Dong, L. Jiang, W. Hu, *Chem. Soc. Rev.* **2018**, *47*, 422 – 500.

[3] a) J. Hou, O. Inganäs, R. H. Friend, F. Gao, *Nat. Mater.* **2018**, *17*, 119; b) R. Noriega, J. Rivnay, K. Vandewal, F. P. V. Koch, N. Stingelin, P. Smith, M. F. Toney, A. Salleo, *Nat. Mater.* **2013**, *12*, 1038; c) J. Mei, Y. Diao, A. L. Appleton, L. Fang, Z. Bao, *J. Am. Chem. Soc.* **2013**, *135*, 6724 – 6746; d) X. Guo, A. Facchetti, T. J. Marks, *Chem. Rev.* **2014**, *114*, 8943 – 9021; e) H. Zang, Y. Liang, L. Yu, B. Hu, *Adv. Energy Mater.* **2011**, *1*, 923 – 929.

[4] J. L. Brédas, J. P. Calbert, D. A. da Silva Filho, J. Cornil, *Proc. Natl. Acad. Sci. USA* **2002**, *99*, 5804 – 5809.

[5] a) S. Wu, M. T. Gonzalez, R. Huber, S. Grunder, M. Mayor, C. Schoenenberger, M. Calame, *Nat. Nanotechnol.* **2008**, *3*, 569 – 574; b) S. Martín, I. Grace, M. R. Bryce, C. Wang, R. Jitchati, A. S. Batsanov, S. J. Higgins, C. J. Lambert, R. J. Nichols, *J. Am. Chem. Soc.* **2010**, *132*, 9157 – 9164.

[6] a) A. Mishra, C.-Q. Ma, J. L. Segura, P. Bäuerle, *Handbook of Thiophene-Based Materials*, Wiley, Hoboken, **2009**, pp. 1 – 155; b) M. E. Cinar, T. Ozturk, *Chem. Rev.* **2015**, *115*, 3036 – 3140; c) J.-S. Ni, P. Zhang, T. Jiang, Y. Chen, H. Su, D. Wang, Z.-Q. Yu, R. T. K. Kwok, Z. Zhao, J. W. Y. Lam, B. Z. Tang, *Adv. Mater.* **2018**, *30*, 1805220.

[7] a) L. Xiang, T. Hines, J. L. Palma, X. Lu, V. Mujica, M. A. Ratner, G. Zhou, N. Tao, *J. Am. Chem. Soc.* **2016**, *138*, 679 – 687; b) B. Capozzi, E. J. Dell, T. C. Berkelbach, D. R. Reichman, L. Venkataraman, L. M. Campos, *J. Am. Chem. Soc.* **2014**, *136*, 10486 – 10492; c) S. K. Lee, R. Yamada, S. Tanaka, G. S. Chang, Y. Asai, H. Tada, *ACS Nano* **2012**, *6*, 5078 – 5082; d) B. Q. Xu, X. L. Li, X. Y. Xiao, H. Sakaguchi, N. J. Tao, *Nano Lett.* **2005**, *5*, 1491 – 1495; e) E. Leary, H. Höbenreich, S. J. Higgins, H. van Zalinge, W. Haiss, R. J. Nichols, C. M. Finch, I. Grace, C. J. Lambert, R. McGrath, J. Smerdon, *Phys. Rev. Lett.* **2009**, *102*, 086801.

[8] A. I. Yanson, G. R. Bollinger, H. E. van den Brom, N. Agraït, J. M. van Ruitenbeek, *Nature* **1998**, *395*, 783.

[9] a) M. Wawrzyniak, J. Martinek, B. Susla, G. Ilnicki, *Acta Phys. Pol. A* **2009**, *115*, 384 – 386; b) A. Halbritter, P. Makk, S. Mackowiak, S. Csonka, M. Wawrzyniak, J. Martinek, *Phys. Rev. Lett.* **2010**, *105*, 266805; c) A. Mishchenko, L. A. Zotti, D. Vonlanthen, M. Bürkle, F. Pauly, J. C. Cuevas, M. Mayor, T. Wandlowski, *J. Am. Chem. Soc.* **2011**, *133*, 184 – 187; d) P. Makk, D. Tomaszewski, J. Martinek, Z. Balogh, S. Csonka, M. Wawrzyniak, M. Frei, L. Venkataraman, A. Halbritter, *Acs Nano* **2012**, *6*, 3411 – 3423.

[10] A. C. Aragonès, N. Darwish, J. Im, B. Lim, J. Choi, S. Koo, I. Díez-Pérez, *Chem. Eur. J.* **2015**, *21*, 7716 – 7720.

[11] C. R. Arroyo, S. Tarkuc, R. Frisenda, J. S. Seldenthuis, C. H. M. Woerde, R. Eelkema, F. C. Grozema, H. S. J. van der Zant, *Angew. Chem. Int. Ed.* **2013**, *52*, 3152 – 3155; *Angew. Chem.* **2013**, *125*, 3234 – 3237.

[12] W. Hong, D. Z. Manrique, P. Moreno-Garcia, M. Gulcur, A. Mishchenko, C. J. Lambert, M. R. Bryce, T. Wandlowski, *J. Am. Chem. Soc.* **2012**, *134*, 2292 – 2304.

[13] a) A. Magyarkuti, O. Adak, A. Halbritter, L. Venkataraman, *Nanoscale* **2018**, *10*, 3362 – 3368; b) M. H. Garner, H. Li, Y. Chen, T. A. Su, Z. Shangguan, D. W. Paley, T. Liu, F. Ng, H. Li, S. Xiao, C. Nuckolls, L. Venkataraman, G. C. Solomon, *Nature* **2018**, *558*, 415.

[14] R. Gleiter, G. Haberhauer, D. B. Werz, F. Rominger, C. Bleiholder, *Chem. Rev.* **2018**, *118*, 2010 – 2041.

[15] S. K. Rajagopal, P. S. Salini, M. Hariharan, *Cryst. Growth Des.* **2016**, *16*, 4567 – 4573.

[16] S. A. Lee, S. Hotta, F. Nakanishi, *J. Phys. Chem. A* **2000**, *104*, 1827 – 1833.

[17] M. Carini, M. P. Ruiz, I. Usabiaga, J. A. Fernández, E. J. Cocinero, M. Melle-Franco, I. Diez-Perez, A. Mateo-Alonso, *Nat. Commun.* **2017**, *8*, 15195.

[18] A. R. Rocha, V. M. García-suárez, S. W. Bailey, C. J. Lambert, J. Ferrer, S. Sanvito, *Nat. Mater.* **2005**, *4*, 335.

[19] J. Ferrer, C. J. Lambert, V. M. Garcia-Suarez, D. Z. Manrique, D. Visontai, L. Oroszlany, R. Rodriguez-Ferradas, I. Grace, S. W. D. Bailey, K. Gillemot, H. Sadeghi, L. A. Algharagholy, *New J. Phys.* **2014**, *16*, 093029.
[20] R. Frisenda, V. A. E. C. Janssen, F. C. Grozema, H. S. J. van der Zant, N. Renaud, *Nat. Chem.* **2016**, *8*, 1099 – 1104.
[21] M. K. Al-Khaykanee, A. K. Ismael, I. Grace, C. J. Lambert, *RSC Adv.* **2018**, *8*, 24711 – 24715.

Manuscript received: October 18, 2019
Accepted manuscript online: December 5, 2019
Version of record online: ■■ ■■, ■■■■

Research Articles

Charge Transport

X. H. Li, Q. Q. Wu, J. Bai, S. J. Hou, W. L. Jiang, C. Tang, H. Song, X. J. Huang, J. T. Zheng, Y. Yang, J. Y. Liu, Y. Hu, J. Shi, Z. T. Liu,* C. J. Lambert,* D. Q. Zhang,* W. J. Hong* ——— ■■■–■■■

Structure-Independent Conductance of Thiophene-Based Single-Stacking Junctions

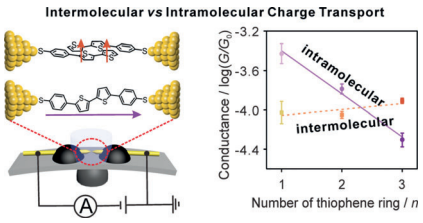

Which mode of transport? The conductance of thiophene-based single-stacking junctions was found to be nearly independent of the conjugation pattern of the molecular structure. When the length of the conjugated region increased, there was a change in the dominant charge-transport path from intramolecular to intermolecular (see picture).